

AD-A036 331

AIR FORCE GEOPHYSICS LAB HANSCOM AFB MASS
HIGH-RESOLUTION SPECTRA OF CH4 IN THE 2700 TO 3200 CM-1 REGION. (U)

F/G 7/4

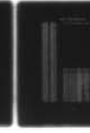
NOV 76 H SAKAI

UNCLASSIFIED

AFGL-TR-76-0280

NL

| OF |
AD
A036331



END

DATE
FILMED

3-77

12
B5
ADA036331

AFGL-TR-76-0280
ENVIRONMENTAL RESEARCH PAPERS, NO. 584



High-Resolution Spectra of CH₄ in the 2700 to 3200 cm⁻¹ Region

HAJIME SAKAI

29 November 1976

D D C
DRAFTED
MAR 4 1977
RECEIVED
C
J

Approved for public release; distribution unlimited.

OPTICAL PHYSICS DIVISION PROJECT 2310
AIR FORCE GEOPHYSICS LABORATORY
HANSCOM AFB, MASSACHUSETTS 01731

AIR FORCE SYSTEMS COMMAND, USAF





This report has been reviewed by the ESD Information Office (OI) and is releasable to the National Technical Information Service (NTIS).

This technical report has been reviewed and is approved for publication.

FOR THE COMMANDER

John Howard
Chief Scientist

Qualified requestors may obtain additional copies from the Defense Documentation Center. All others should apply to the National Technical Information Service.

Unclassified

SECURITY CLASSIFICATION OF THIS PAGE (When Data Entered)

REPORT DOCUMENTATION PAGE		READ INSTRUCTIONS BEFORE COMPLETING FORM
1. REPORT NUMBER <i>(14) AFGL-TR-76-0280</i>	2. GOVT. ACCESSION NO. <i>AFGL-ERP-584</i>	3. RECIPIENT'S CATALOG NUMBER
4. TITLE (and Subtitle) <i>HIGH-RESOLUTION SPECTRA OF CH₄ IN THE 2700 to 3200 cm⁻¹ REGION</i>		5. TYPE OF REPORT & PERIOD COVERED <i>Scientific. Interim.</i>
6. AUTHOR(s) <i>(10) Hajime Sakai</i>		7. PERFORMING ORGANIZATION NAME AND ADDRESS <i>Air Force Geophysics Laboratory (OPI) Hanscom AFB, Massachusetts 01731</i>
8. CONTRACT OR GRANT NUMBER(s) <i>(11) 13121p.</i>		9. PROGRAM ELEMENT, PROJECT, TASK AREA & WORK UNIT NUMBERS <i>(16) 61102F 2310G101 (17) G1</i>
10. REPORT DATE <i>(11) 29 Nov 1976</i>		11. NUMBER OF PAGES <i>20</i>
12. MONITORING AGENCY NAME & ADDRESS (if different from Controlling Office) <i>(9) Environmental Research Papers</i>		13. SECURITY CLASS. (of this report) <i>Unclassified</i>
14. DISTRIBUTION STATEMENT (of this Report) <i>Approved for public release; distribution unlimited.</i>		15. DECLASSIFICATION/DOWNGRADING SCHEDULE
16. DISTRIBUTION STATEMENT (of the abstract entered in Block 20, if different from Report)		
17. SUPPLEMENTARY NOTES		
18. KEY WORDS (Continue on reverse side if necessary and identify by block number) <i>Methane Fourier Spectroscopy</i>		
19. ABSTRACT (Continue on reverse side if necessary and identify by block number) <i>The Idealab 2-m path-difference interferometer was used to obtain data of CH₄ in the 2700 to 3200 cm⁻¹ region to a resolution of 0.006 cm⁻¹. Obtained spectral data are presented as well as the results of analysis to calculate line positions and strengths. A comparison of the present data with previously obtained data is also presented. The results of this study are tabulated using the format of the AFGL atmospheric line compilation.</i>		

DD FORM 1 JAN 73 EDITION OF 1 NOV 65 IS OBSOLETE

Unclassified
SECURITY CLASSIFICATION OF THIS PAGE (When Data Entered)

* 1/2700 to 1/3200 cm

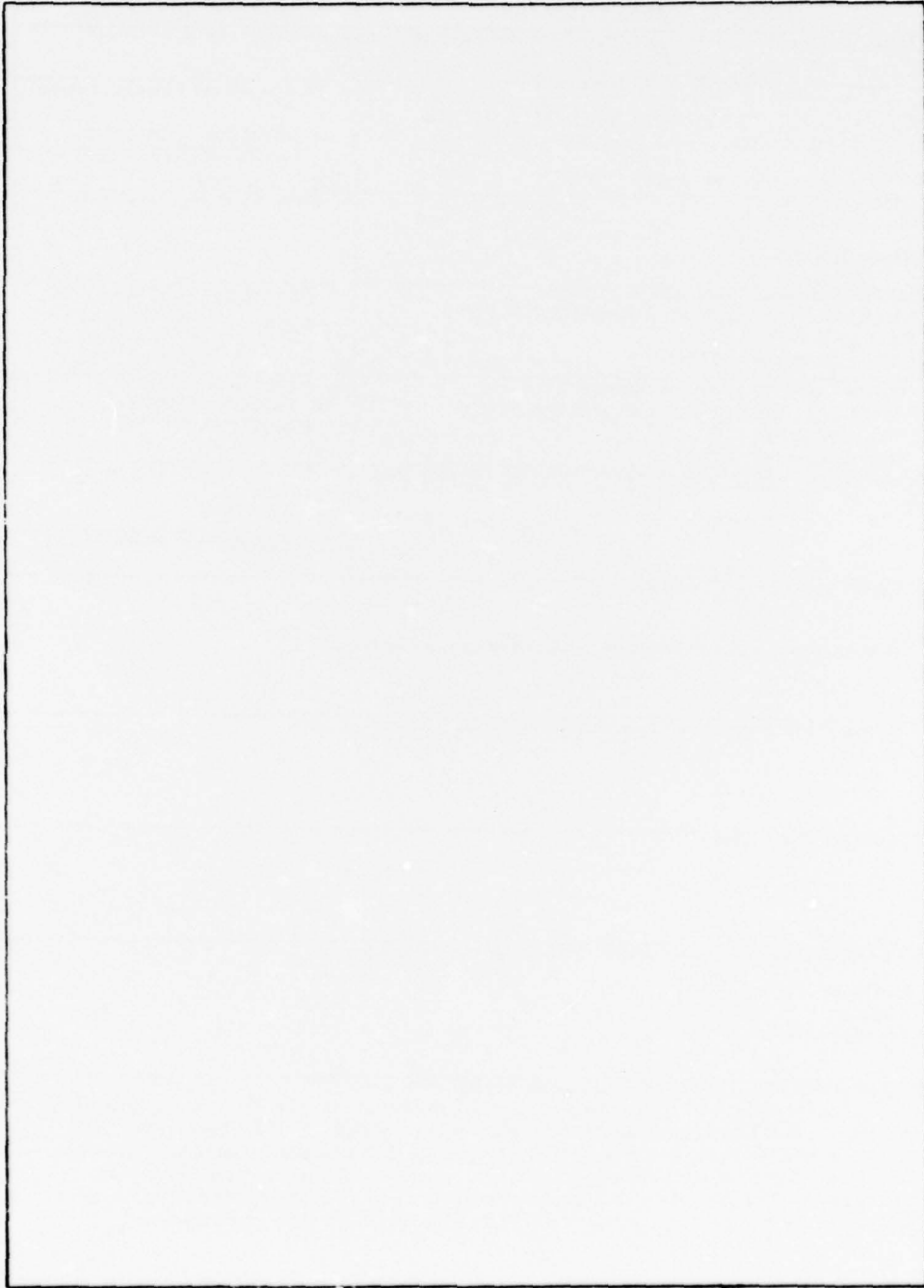
1.006 cm

409 578

N

Unclassified

SECURITY CLASSIFICATION OF THIS PAGE(When Data Entered)



Unclassified

SECURITY CLASSIFICATION OF THIS PAGE(When Data Entered)

Contents

1. INTRODUCTION	5
2. EXPERIMENTAL PART	6
3. DATA ANALYSIS	9
4. RESULTS AND DISCUSSION	13
REFERENCES	20

Illustrations

1. Optical Layout of Interferometer and Its Auxiliary Optics	7
2. Block Diagram of Data Acquisition System	8
3. Raw Methane Absorption Spectrum	9
4. Flow Diagram of Spectral Data Analysis	10
5. CH_4 Absorptance Spectrum	10
6. Comparison of Observed CH_4 Absorptance Spectrum With Synthetic Spectrum Calculated Using the Line Parameters Derived From Present Analysis	12
7. Comparison of Observed CH_4 Absorptance Spectrum With Synthetic Spectrum Calculated Using the Line Parameters Compiled by Fox	12

Tables

1. Summary of the Data Runs Taken for Various Methane Pressures	9
2. Results Obtained	14
3. The Lines Unanalyzed Because of a Severe Blending	19

High-Resolution Spectra of CH_4 In the 2700 to 3200 cm^{-1} Region

I. INTRODUCTION

The AFGL atmospheric line compilation contains the line parameters of the infrared methane bands.¹ The work on methane was started by Kyle and later revised by Fox.² The compilation of methane is rather extensive, covering most of the major infrared bands; however, it is still considered incomplete. The most intense band of methane in the infrared region is the so-called ν_3 band (00011001 - 00000000 transition according to the designation used in the AFGL line compilation) of C^{12}H_4 , extending in spectral range from 2700 cm^{-1} to 3200 cm^{-1} . The line data for this band are compiled from both existing experimental data and theoretical analysis. Other methane bands, which are weaker than the ν_3 band of C^{12}H_4 but make a significant contribution to infrared absorption in this region, are the ν_3 of C^{13}H_4 (00011001 - 00000000) and the ($\nu_2 + \nu_4$) of C^{12}H_4 (0110112 - 00000000). The calculated strength of lines in these bands, which are in the compilation, ranges from 10^{-23} to 2×10^{-19} in units of $\text{cm}^{-1}/(\text{molecules cm}^{-2})$.

The methane spectrum in this spectral range (2700 \rightarrow 3200 cm^{-1}) exhibits a somewhat complex structure. If the spectroscopic measurement is made to resolve

(Received for publication 24 November 1976)

1. McClatchey et al (1973) AFCRL Atmospheric Absorption Line Parameters Compilation, AFCRL-TR-~~73-0096~~.
2. Fox, K. (1973) Analysis of Vibration-Rotation Spectra of Methane, AFCRL-TR-73-0738.

all the spectral lines, the resolution of the spectrometer must be at least as fine as the Doppler width of these lines, that is, 0.0047 cm^{-1} . Our 2-m path-difference interferometer spectrometer^{3,4} is capable of producing the required resolution. The present work was accomplished to achieve two goals: testing the performance capability of our interferometer, and examining the line parameters compiled for the $3-\mu$ methane lines in the AFGL atmospheric line compilation.

Traditionally, the spectral analysis has been mainly concerned with the determination of line positions in the measured spectral band. On the other hand, very little has been done in the way of analysis of measured line strengths and widths of individually measured lines. The present work was undertaken to devise an automatic computation program for analyzing line strengths and widths as well as for determining line positions.

2. EXPERIMENTAL PART

The interferometer spectrometer used for the present measurement has been described in previous reports, together with the scheme for recording the interferogram function.^{3,4} The computational method used in processing the interferogram data to obtain the spectrum was also described in the above reports; consequently, no detailed description of it will be presented here. The description that follows highlights those features that are pertinent to the present specific measurement.

The interferometer, with its auxiliary optical components, is housed in a vacuum chamber. Figure 1 is a schematic diagram showing the arrangement. The radiation from the primary source, which is a small tungsten-filament incandescent lamp GE 51, is first focused on a blade of a vibrating reed chopper driven at a rate of 450 Hz. A spectral bandpass filter is placed between the source and the chopper to isolate the spectral region of interest. The chopped beam is refocused at the 1-mm-diam entrance aperture, and then collimated using all-reflecting optics. A 10-cm-long absorption cell, made of fused quartz, is placed before the interferometer and in the path of the collimated beam. Two PbS detectors operating at liquid nitrogen temperature are placed at both output ends of the interferometer to observe the complementary modulations of the interferogram signals. The 6329 Å line from the frequency-stabilized He-Ne cw laser supplies the reference signal used to control the interferometer stepping and the interferogram data sampling. No correction is needed to the measured line position, since the whole

3. Pritchard et al (1973) Two-Meter Path Difference Interferometer for Fourier Spectroscopy, AFCRL-TR-73-0223.
4. Sakai, H. (1974) High-Resolution Fourier Spectroscopy, AFCRL-TR-74-0571.

interferometer system is under vacuum and the atmosphere does not influence the calibration.

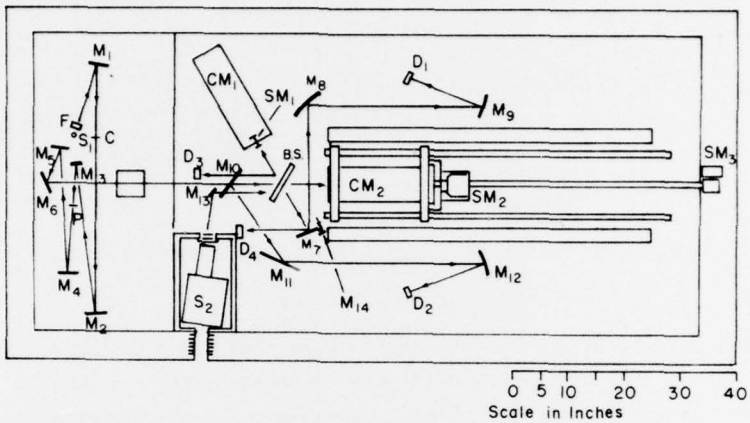


Figure 1. Optical Layout of Interferometer and its Auxiliary Optics. CM₁: stationary cat's eye; CM₂: movable cat's eye; SM₁: piezo-electric crystal transducer; SM₂: magnetic motor; SM₃: printed circuit motor; S₁: signal sources; S₂: reference laser; C: chopper; F: filter; P: entrance hole; D₃ and D₄: interference fringe signal detectors; B.S.: beam splitter plate; D₁ and D₂: interferogram signal detectors; M_s: mirrors

The scheme used for recording the interferogram data is shown in Figure 2. The detectors are carefully positioned to produce optimum balance of their output modulations. After these outputs are individually amplified, they are subtracted from each other to yield an interferogram signal that is modulated about zero voltage. An analog phase-adjusting circuit is inserted in one channel, prior to the differencing amplifier, to improve signal balancing. An analog-to-digital converter is used to convert the interferogram signal into a series of digital numbers. The PDP 8e minicomputer performs the arithmetic operations on these digitized values, the operations being equivalent to synchronous demodulation and integration. The interferogram data thus obtained are recorded on digital magnetic tape and processed at the central-site large-scale CDC 6600 computer. The overall dynamic range in this recording scheme is better than 18 bits (approximately 2.6×10^5).

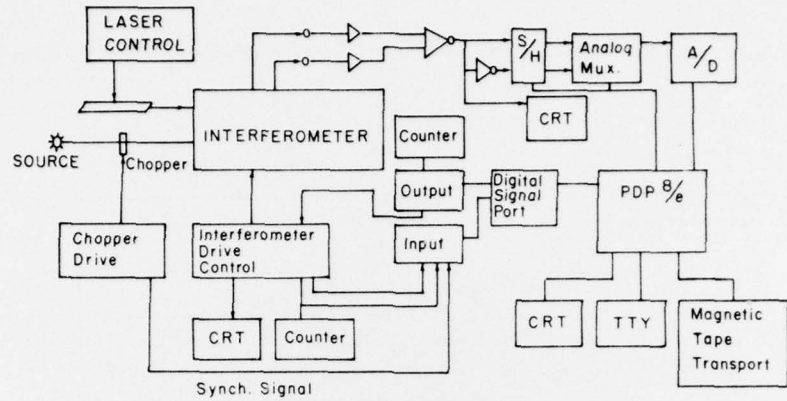


Figure 2. Block Diagram of Data Acquisition System

The methane gas used in the present measurement was of Linde cp grade. The amount of methane in the absorption cell was measured using a Texas Instrument quartz spiral pressure gauge and an oil manometer. The stepping distance of the interferometer was set to twice the wavelength of the He-Ne laser line, which means that the interferogram signal was sampled at every $2 \times 6329.9 \text{ \AA} = 12659.8 \text{ \AA}$. The measurement of a complete interferogram took about 10 hr, covering an optical path difference of 100 cm. The hold time of the liquid-nitrogen-detector dewar limits the total measurement time to about 10 hr. The measurements were carried out either at night on workdays or on weekends, in order to avoid the harmful disturbances that we cannot eliminate under normal workday conditions.

The spectral range covered in a single measurement was approximately from 2700 cm^{-1} to 3200 cm^{-1} . As mentioned above, a spectral bandpass filter was used to isolate this spectral region. The recorded interferogram contained about 10^6 data points, which is considerably more than necessary to satisfy the sampling theorem.

Figure 3 shows typical methane spectral data obtained by Fourier-transforming the recorded interferogram data. The spectrum represents the Q branch region of the $\text{C}^{12}\text{H}_4 \nu_3$ band. The periodic modulation of the peak power observed in the spectrum is channelled spectrum, caused by the spectral bandpass filter. The spectral resolution, which corresponds to the distance between adjacent independent spectral data points, is 0.006 cm^{-1} , corresponding to a maximum optical path difference of 90 cm. Table 1 summarizes the experimental conditions under which data were taken for the present analysis.

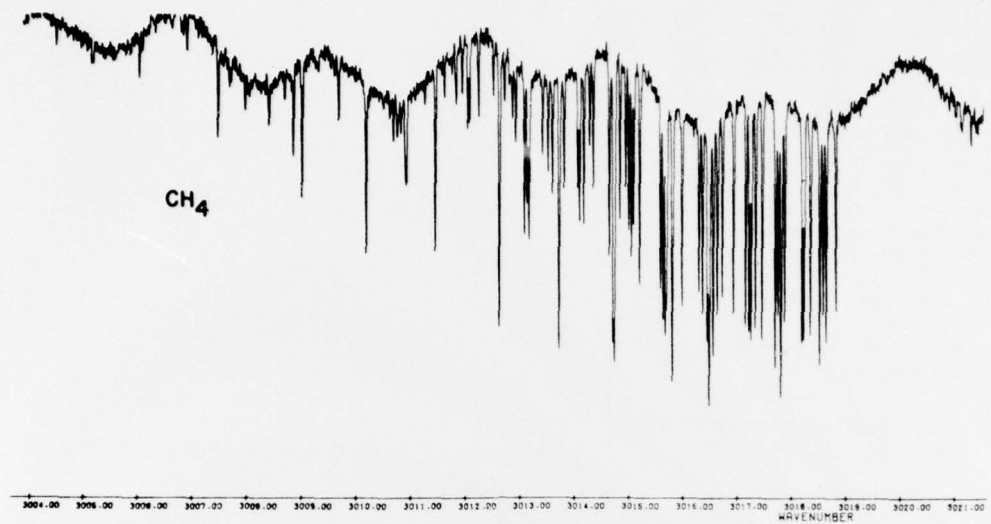


Figure 3. Raw Methane Absorption Spectrum

Table 1. Summary of the Data Runs Taken for Various Methane Pressures
(Absorption cell length = 10 cm)

Methane Pressure in mm Hg	No. of Runs
1.0	4
1.6	4
2.5	1
2.7	6
9.0	1
21.0	1

3. DATA ANALYSIS

Analysis of the spectral data was carried out according to the sequence shown in the flow diagram of Figure 4. The absorptance spectrum produced by the first stage program is shown in Figure 5. In the next stage the positions of all absorption peaks were determined to an accuracy better than 1/8 of the spectral resolution. The last stage of the sequence was to determine the strengths and widths of all observed lines, using the least-square-error curve-fitting algorithm. In constructing the last stage algorithm, the following assumptions were made: (1) the lines may be characterized as having a Doppler-broadened Gaussian shape; (2) all lines are free of severe overlapping so that the observed peaks correspond to the centers

of the lines; and (3) all lines are not strongly saturated at their absorption peaks. The algorithm was able to produce the strengths and widths of each constituent line, even in the case where the lines being analyzed overlapped somewhat.

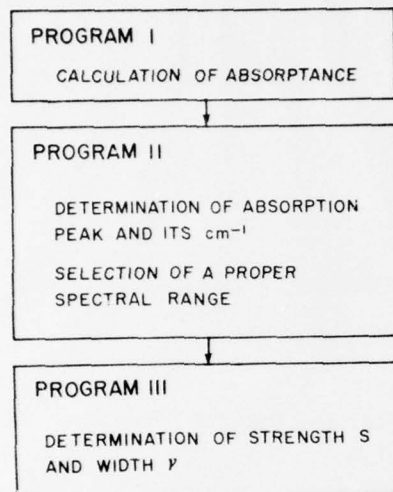


Figure 4. Flow Diagram of Spectral Data Analysis

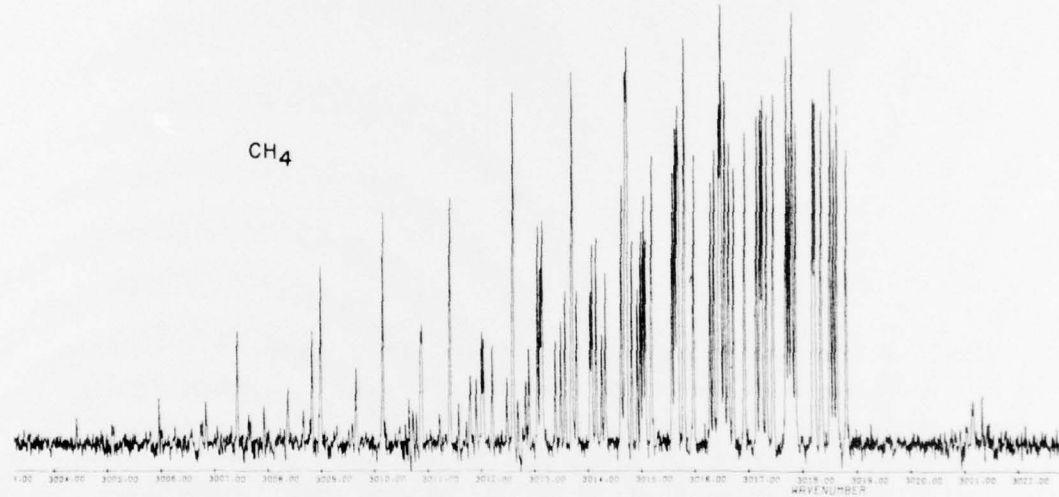


Figure 5. CH₄ Absorptance Spectrum

The first assumption is considered appropriate, since the pressure ranges used for all the measurements were quite low. The intermolecular collisions in those pressure ranges do not produce any significant line broadening. The widths determined for most of the data were not too different from the theoretically calculated value of 0.0047 cm^{-1} . Thus, there is no indication of inconsistency between the assumptions and the results obtained.

The second assumption can be tested by examining the widths determined from the analysis. An unusually large value of line widths compared with those determined for neighboring lines would indicate the presence of hidden lines, even if the observed data suggest a single line. This was not the case for most of the data observed, except for the forbidden Q^+ branch where the blending is quite severe.

The third assumption is the most crucial one for deciding on the applicability of the algorithm. It was found that the algorithm failed to produce a unique set of solutions for the strengths and widths of lines that are too strong. Once the absorption coefficient at the line center exceeds a certain threshold value, interdependency between these two parameters becomes too high to allow independent determination of the strength and width. Iterative application of the least-square curve-fitting computation for this case fails to produce a convergent set of solutions. This difficulty can be avoided by selecting the appropriate range of pressures for the analysis of individual lines. The stronger lines were analyzed using the low pressure data, while the weaker lines were processed using the high pressure data.

The line parameter data produced from data from each interferogram were normalized according to the methane concentration present in the absorption cell. The data obtained from all interferograms were collected for the individual lines and averaged. Figure 6 shows a comparison between one of the observed absorptance spectrum and the spectrum calculated for the same methane concentration using the line parameters resulting from analysis of the present data. The agreement between these two spectra is adequate to conclude that the line parameters determined in this work are acceptable and within experimental error for the present measurement.

Figure 7 shows a comparison between the observed absorptance spectrum and that synthesized from the line parameters compiled by Fox. It can be seen that the band head section of the Q branch shows satisfactory agreement. Discrepancy between these two spectra is noticeable, however, in the region below 3013 cm^{-1} , where the lines are due to transitions between levels corresponding to high rotational quantum numbers.

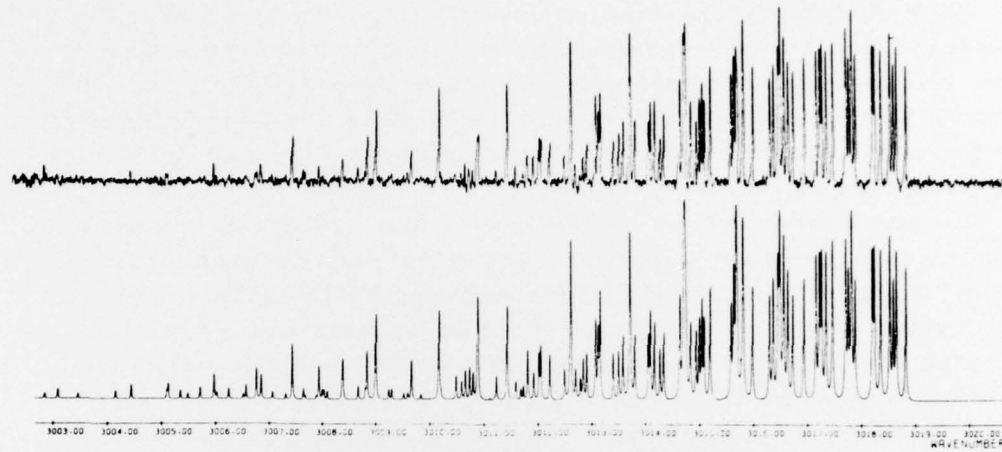


Figure 6. Comparison of Observed CH₄ Absorptance Spectrum With Synthetic Spectrum Calculated Using the Line Parameters Derived From Present Analysis

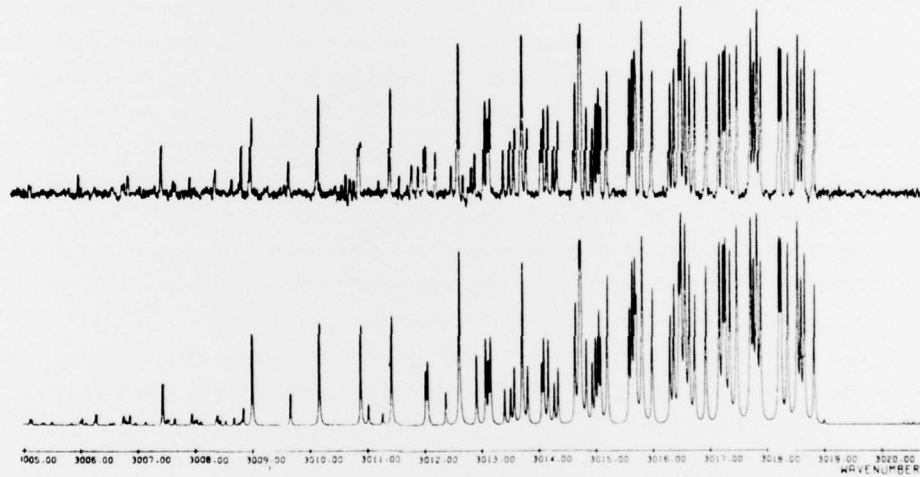


Figure 7. Comparison of Observed CH₄ Absorptance Spectrum With Synthetic Spectrum Calculated Using the Line Parameters Compiled by Fox

4. RESULTS AND DISCUSSION

The results of this study are listed in Table 2, using the format of the AFGL atmospheric line compilation (F10.3, E10.3, F5.3, F10.3, 2A9, 2A8, 2I4, I3). The lines are usually identified according to the line listing compiled by Fox. Values for the widths are left blank, since the present work essentially only measured the Doppler-broadened width. As indicated in Figure 7, the line compilation for the spectral range of 3000 cm^{-1} to 3013 cm^{-1} is unsatisfactory. Of the lines observed in this spectral range, identification is assigned only to those lines that show good agreement with the line compilation. The unidentified lines show a blank space between column 27 and 77. The values of the lower energy levels in the present list are taken from the recent French work.⁵ The internal identification code that appears from column 81 through 84 is 36 for the present result. The lines for the forbidden Q⁺ branch in the range around 3020 cm^{-1} are those compiled by Fox, and are indicated by the code 73. The analysis of these lines was not attempted because of their severe overlapping. Several other C¹²H₄ lines of the ν_3 band are also left unanalyzed, because of the same difficulty. Those lines are listed in Table 3.

After the major portion of the present work had been completed, but before this report was written, work by Pine was published.⁶ He measured the major C¹²H₄ lines of the ν_3 band between 2916 cm^{-1} and 3123 cm^{-1} using the tunable laser technique. The spectral resolution that he attained using the laser technique is better than 10^{-4} cm^{-1} . The signal-to-noise ratio of his measurement is significantly better than that of the present measurement. The line strength values obtained by Pine for those lines are slightly higher than the values compiled by Fox (about 20 to 30 percent), while the values obtained by the present work average around the Fox values.

5. Tarrago et al (1976) J. Mol. Spectrosc., 57:246.

6. Pine, A.S. (1976) J. Opt. Soc. Am., 66:97.

Table 2. Results Obtained

2894.994	.131E-19	815.144	00 11001 000000_0	1112A21	1412A11	36	211	6
2895.057	.573E-20	815.132	00 11001 000000_0	1112F21	1412F11	36	211	6
2895.129	.554E-20	815.116	00 11001 000000_0	1112F11	1412F21	36	211	6
2895.233	.120E-19	815.089	00 11001 000000_0	1112A11	1412A21	36	211	6
2895.759	.120E-19	815.088	00 11001 000000_0	1112F12	1412F22	36	211	6
2895.827	.440E-20	814.993	00 11001 000000_0	1112 E1	1412 E1	36	211	6
2896.202	.570E-20	814.894	00 11001 000000_0	1112F22	1412F12	36	211	6
2896.308	.100E-19	814.847	00 11001 000000_0	1112F13	1412F23	36	211	6
2896.983	.329E-19							6
2897.404	.150E-20	62.875	01100112 000000_0	4 3A11	3 3A21	36	211	6
2898.695	.110E-20	62.876	01100112 000000_0	4 3F21	3 3F11	36	211	6
2899.323	.120E-20							6
2899.932	.910E-21							6
2900.119	.840E-20	62.875	01100112 000000_0	4 3A11	3 3A21	36	211	6
2901.539	.214E-20	62.876	01100112 000000_0	4 3F21	3 3F11	36	211	6
2901.887	.329E-20							6
2903.872	.690E-21							6
2904.529	.940E-21							6
2905.633	.120E-19	690.049	00 11001 000000_0	1011F23	1411F13	36	211	6
2905.699	.671E-20	690.040	00 11001 000000_0	1011 F2	1411 E2	36	211	6
2905.813	.170E-19	690.018	00 11001 000000_0	1011F13	1411F23	36	211	6
2906.093	.693E-21	575.223	00 11001 000000_0	910A21	1410A11	36	311	6
2906.282	.131E-19	689.957	00 11001 000000_0	1011F22	1411F12	36	211	6
2906.589	.943E-20	689.820	00 11001 000000_0	1011 E1	1411 E1	36	211	6
2906.649	.137E-19	689.877	00 11001 000000_0	1011F22	1411F22	36	211	6
2906.732	.187E-19	689.842	00 11001 000000_0	1011A11	1411A21	36	211	6
2907.325	.310E-19							6
2908.331	.214E-20							6
2909.273	.250E-20							6
2909.884	.147E-20							6
2910.554	.301E-20							6
2910.812	.730E-21							6
2913.789	.824E-21							6
2914.921	.603E-21							6
2916.001	.304E-20							6
2916.007	.214E-20							6
2916.201	.150E-19	575.295	00 11001 000000_0	910F11	1410F21	36	211	6
2916.302	.127E-19	575.272	00 11001 000000_0	910 F1	1410 E1	36	211	6
2916.395	.274E-19	575.260	00 11001 000000_0	910F21	1410F11	36	211	6
2916.524	.180E-20							6
2916.753	.265E-19	575.223	00 11001 000000_0	910A21	1410A11	36	211	6
2916.966	.187E-19	575.124	00 11001 000000_0	910F22	1410F12	36	211	6
2917.066	.214E-19	575.170	00 11001 000000_0	910F12	1410F22	36	211	6
2917.632	.280E-19	575.050	00 11001 000000_0	910A11	1410A21	36	211	6
2918.485	.143E-21							6
2918.735	.357E-20							6
2919.132	.704E-20							6
2919.891	.109E-20							6
2920.195	.510E-21							6
2920.616	.710E-21							6
2920.666	.120E-20							6
2921.333	.952E-21							6
2922.911	.531E-21							6
2923.949	.260E-21							6
2926.700	.504E-19	470.973	00 11001 000000_0	8 9A11	14 9A21	36	211	6
2926.782	.241E-19	470.865	00 11001 000000_0	8 9F12	14 9F22	36	211	6
2926.882	.237E-19	470.855	00 11001 000000_0	8 9F23	14 9F13	36	211	6
2927.075	.440E-19	470.871	00 11001 000000_0	8 9A21	14 9A11	36	211	6
2927.372	.233E-19	470.875	00 11001 000000_0	8 9F22	14 9F12	36	211	6
2927.429	.188E-19	470.799	00 11001 000000_0	8 9 F1	14 9 E1	36	211	6

Table 2. Results Obtained (Cont)

2947.044	.475E-21	37~.730 00 14~01 000000_0	7 8A12	5 8A11	36 211	5
2947.932	.33~E-19	47~.720 00 14~01 000000_0	5 9F11	5 9F21	36 211	5
2947.954	.24~E-19	47~.717 00 14~01 000000_0	5 9F21	5 9F11	36 211	5
2947.744	.275E-21	47~.719 00 14~01 000000_0	5 5F22	5 5F12	36 211	5
2947.762	.240E-21	37~.714 00 14~01 000000_0	7 7F21	5 8F12	36 211	5
2947.972	.175E-21					5
2947.023	.347E-21					5
2947.251	.171E-21	157~.137 01~00~12 000000_0	5 5 F1	5 5 E1	36 211	5
2947.851	.303E-21	157~.128 01~00~12 000000_0	5 5F11	5 5F21	36 211	5
2947.247	.317E-21	157~.124 01~00~12 000000_0	5 5F21	5 5F11	36 211	5
2947.234	.464E-19	37~.510 00~14~01 000000_0	7 8F11	5 8F21	36 211	6
2947.372	.202E-14	37~.521 00~14~01 000000_0	7 8 F1	5 8 E1	36 211	6
2947.494	.354E-19	37~.5 00~14~01 000000_0	7 HF21	5 8F11	36 211	6
2947.657	.220E-21	27~.14 00 14~01 000000_0	6 7A11	7 7A21	36 311	6
2947.756	.302E-19	37~.740 00 14~01 000000_0	7 HF12	5 8F22	36 211	6
2947.912	.304E-21	27~.120 00 14~01 000000_0	5 7F11	7 7F21	36 311	6
2947.967	.304E-21	27~.123 00 14~01 000000_0	5 7F21	7 7F11	36 311	6
2947.192	.450E-19	37~.735 00 14~01 000000_0	7 8 E2	5 8 E2	36 211	6
2947.614	.594E-19	37~.747 00 14~01 000000_0	7 8F12	5 8F12	36 211	6
2947.257	.494E-19	37~.730 00 14~01 000000_0	7 8A21	5 8A11	36 211	6
2947.127	.720E-21					6
2947.247	.634E-21					6
2947.332	.244E-21					6
2947.617	.240E-21					6
2947.871	.860E-21					6
2947.647	.580E-21					6
2947.943	.410E-21					6
2947.002	.954E-22					6
2947.427	.152E-21					6
2947.657	.504E-19	293~.178 00 14~01 000000_0	5 7F22	7 7F12	36 211	6
2947.811	.303E-19	293~.170 00 14~01 000000_0	5 7 F1	7 7 E1	36 211	6
2947.912	.507E-19	293~.144 00 14~01 000000_0	5 7F12	7 7F22	36 211	6
2947.107	.100E-18	293~.154 00 14~01 000000_0	5 7A11	7 7A21	36 211	6
2947.232	.410E-21					6
2947.427	.577E-19	293~.126 00 14~01 000000_0	5 7F11	7 7 F1	36 211	6
2947.474	.450E-19	293~.123 00 14~01 000000_0	5 7F21	7 7F11	36 211	6
2947.020	.417E-21					6
2947.122	.244E-21					6
2947.347	.400E-21					6
2947.122	.440E-21					6
2947.192	.544E-20	214~.920 01~00~12 000000_0	7 5A11	5 5A21	36 211	5
2947.534	.327E-20	214~.917 01~00~12 000000_0	7 6F11	5 5F21	36 211	5
2947.687	.197E-20	214~.913 01~00~12 000000_0	7 6 F1	5 6 E1	36 211	5
2947.344	.154E-21					5
2947.455	.930E-21	214~.915 00 14~01 000000_0	5 5F11	5 5F22	36 211	5
2947.017	.100E-18	214~.915 00 14~01 000000_0	5 6A21	5 6A11	36 211	5
2947.127	.660E-19	214~.911 00 14~01 000000_0	5 6F11	5 6F21	36 211	5
2947.232	.600E-19	214~.917 00 14~01 000000_0	5 5F11	5 5F21	36 211	5
2947.427	.340E-21	157~.128 00 14~01 000000_0	4 5F11	5 5F21	36 311	6
2947.534	.100E-18	214~.920 00 14~01 000000_0	5 6A11	5 5A21	36 211	6
2947.651	.737E-19	214~.915 00 14~01 000000_0	5 5F12	5 5F22	36 211	6
2947.682	.190E-19	214~.913 00 14~01 000000_0	5 6 F1	5 6 E1	36 211	6
2947.957	.120E-21					6
2947.864	.107E-20					5
2947.958	.137E-21					5
2947.524	.494E-21					5
2947.865	.517E-21					5
2947.102	.460E-21					5
2947.402	.775E-19	157~.139 00 14~01 000000_0	4 5F22	5 5F12	36 211	6
2947.472	.447E-19	157~.137 00 14~01 000000_0	4 5 F1	5 5 E1	36 211	6

Table 2. Results Obtained (Cont)

2968.73	.770E-19	157.128 00 14004 000000_0	4 5F11	5 5F21	36 211	5
2968.855	.764E-19	157.124 00 14004 000000_0	4 5F21	5 5F11	36 211	6
2971.074	.212E-21	293.120 01.00712 000000_0	8 7F11	7 7F21	36 211	6
2971.243	.214E-21	293.123 01.00712 000000_0	8 7F21	7 7F11	36 211	6
2975.142	.444E-21					6
2976.451	.670E-21					6
2978.649	.103E-18	104.770 00 14004 000000_0	3 4F11	4 4F21	36 211	6
2978.847	.417E-19	104.770 00 14004 000000_0	3 4F11	4 4F21	36 211	6
2978.913	.864E-19	104.775 00 14004 000000_0	3 4F21	4 4F11	36 211	6
2979.016	.147E-18	104.773 00 14004 000000_0	3 4A21	4 4A11	36 211	6
2980.073	.813E-21					6
2981.462	.205E-21					6
2982.633	.167E-21					6
2983.385	.133E-20					6
2987.843	.625E-21					6
2988.795	.114E-18	52.575 00 14004 000000_0	2 3A11	3 3A21	36 211	6
2988.932	.744E-19	52.577 00 14004 000000_0	2 3F11	3 3F21	36 211	6
2989.032	.695E-19	52.575 00 14004 000000_0	2 3F21	3 3F11	36 211	6
2989.083	.294E-21	57.575 01.00712 000000_0	9 9F21	5 4F11	36 211	6
2993.177	.440E-21					6
2994.472	.750E-21					6
2995.666	.100E-20					6
2997.944	.185E-21					6
2998.355	.437E-21					6
2998.943	.480E-19	31.044 00 14004 000000_0	1 2F11	2 2F21	36 211	6
2999.051	.250E-19	31.042 00 14004 000000_0	1 2E1	2 2E1	36 211	6
2999.322	.540E-21					6
3000.293	.765E-21					6
3000.734	.174E-21					6
3002.852	.480E-21					6
3003.097	.129E-21					6
3004.462	.440E-21					6
3004.152	.502E+21					6
3004.452	.195E-21	575.170 00 14004 000000_0	1010F12	1010F22	36 311	6
3004.922	.955E-22	575.223 00 14004 000000_0	1010A21	1010A11	36 311	6
3005.102	.981E-21					6
3005.133	.257E-20					6
3005.352	.110E-21	47.0575 00 14004 000000_0	9 9F21	9 9F12	36 311	6
3005.504	.417E-21	47.0571 00 14004 000000_0	9 9A21	9 9A11	36 311	6
3005.727	.100E-20					6
3005.943	.630E-21	293.0123 00 14004 000000_0	7 7F21	7 7F11	36 311	6
3005.253	.254E-21	37.053.5 00 14004 000000_0	8 8F21	5 4F11	36 311	6
3005.525	.640E-21	37.053.1 00 14004 000000_0	8 8F1	5 8E1	36 311	6
3005.582	.227E-21	37.053.0 00 14004 000000_0	8 8F11	5 4F21	36 311	6
3006.752	.182E-20					6
3006.774	.540E-21					6
3006.852	.385E-20					6
3007.077	.105E-20					6
3007.144	.877E-21	293.178 00 14004 000000_0	7 7F22	7 7F12	36 311	6
3007.444	.149E-19					6
3007.655	.130E-21	214.0915 00 14004 000000_0	5 5A21	5 5A11	36 311	6
3007.691	.304E-21					6
3007.942	.104E-19	104.773 00 14004 000000_0	4 4A21	4 4A11	36 311	6
3008.013	.111E-20	157.159 00 14004 000000_0	5 5F22	5 5F12	36 311	6
3008.032	.974E-21	104.775 00 14004 000000_0	4 4F21	4 4F11	36 311	6
3008.383	.525E-20	104.776 00 14004 000000_0	4 4F1	4 4F21	36 311	6
3008.397	.990E-20	1251.0274 00 14004 000000_0	1515A11	1515A21	36 211	5
3008.541	.295E-21	52.577 00 14004 000000_0	3 3F11	3 3F21	36 311	5
3008.812	.102E-21	31.044 00 14004 000000_0	2 2F11	2 2F21	36 311	5
3008.842	.120E-19					5

Table 2. Results Obtained (Cont)

3009.017	.24E-19	41044E 00 11001 000000_0	0 1F21	4 1F11	36 211	6
3009.253	.190E-20					6
3009.304	.140E-20					6
3009.533	.164E-20					6
3009.607	.114E-20					6
3009.674	.866E-20					6
3009.843	.793E-21					6
3009.894	.470E-21					6
3010.177	.294E-19					6
3010.212	.793E-21					6
3010.493	.193E-21					6
3010.505	.390E-21					6
3010.506	.234E-21					6
3010.673	.516E-21					6
3010.747	.740E-21					6
3010.803	.357E-20					6
3010.887	.164E-19					6
3010.913	.173E-19					6
3011.241	.290E-21					6
3011.435	.457E-19					6
3011.547	.734E-20					6
3011.694	.323E-20					6
3011.779	.207E-20					6
3011.819	.964E-20					6
3011.922	.384E-20					6
3012.023	.104E-19					6
3012.042	.804E-20					6
3012.222	.104E-19					6
3012.302	.470E-20					6
3012.615	.130E-19					6
3012.712	.496E-20					6
3012.744	.343E-20					6
3012.839	.134E+20					6
3012.853	.624E-20					6
3012.914	.744E+20					6
3013.077	.164E-19	689.542 00 11001 000000_0	1111A11	1111A21	36 211	6
3013.127	.234E-19	689.577 00 11001 000000_0	1111F12	1111F22	36 211	6
3013.145	.284E-19					6
3013.409	.880E-20	815.110 00 11001 000000_0	1212F11	1212F21	36 211	6
3013.517	.884E-20	815.124 00 11001 000000_0	1212F21	1212F11	36 211	6
3013.542	.150E-19	815.144 00 11001 000000_0	1212A21	1212A11	36 211	6
3013.805	.100E-19	889.557 00 11001 000000_0	1111F22	1111F12	36 211	6
3014.053	.208E-19	891.018 00 11001 000000_0	1111F13	1111F23	36 211	6
3014.092	.200E-19	575.170 00 11001 000000_0	1010F12	1010F22	36 211	6
3014.171	.194E-19	575.194 00 11001 000000_0	1010F22	1010F12	36 211	6
3014.274	.114E-19	670.040 00 11001 000000_0	1111F2	1111E2	36 211	6
3014.344	.242E-19	670.049 00 11001 000000_0	1111F23	1111F13	36 211	6
3014.641	.254E-19	575.223 00 11001 000000_0	1010A21	1010A11	36 211	6
3014.713	.140E-18	370.770 00 11001 000000_0	9 8A21	9 8A11	36 211	6
3014.832	.173E-19	575.250 00 11001 000000_0	1010F21	1010F11	36 211	6
3014.947	.250E-19	575.272 00 11001 000000_0	1010 F1	1010 E1	36 211	6
3015.001	.100E-19	470.709 00 11001 000000_0	9 9 E1	9 9 E1	36 211	6
3015.05	.284E-19	470.815 00 11001 000000_0	9 9F2	9 9F12	36 211	6
3015.090	.177E-19	575.235 00 11001 000000_0	1010F11	1010F21	36 211	6
3015.202	.513E-19	470.851 00 11001 000000_0	9 9A21	9 9A11	36 211	6
3015.542	.203E-19	470.855 00 11001 000000_0	9 9F2	9 9F13	36 211	6
3015.647	.380E-20	293.123 00 11001 000000_0	7 7F21	7 7F11	36 211	6
3015.694	.927E-19	293.126 00 11001 000000_0	7 7F11	7 7F21	36 211	6
3015.949	.504E-19	370.535 00 11001 000000_0	8 8F21	8 8F11	36 211	6
3016.301	.263E-19	370.541 00 11001 000000_0	8 8 E1	9 9 E1	36 211	6

Table 2. Results Obtained (Cont)

3016.369	.389E-19	376.820 00 14004 000000_0	3 5F11	5 9F21	36 211	5
3016.458	.590E-19	249.913 00 14004 000000_0	5 5 F1	5 5 F1	36 211	5
3016.565	.147E-19	249.920 00 14004 000000_0	6 6A1	5 5A21	36 211	5
3016.648	.617E-19	293.164 00 14004 000000_0	7 7F12	7 7F22	36 211	5
3016.733	.447E-19	293.170 00 14004 000000_0	7 7 F1	7 7 F1	36 211	5
3016.945	.710E-19	293.178 00 14004 000000_0	7 7F22	7 7F12	36 211	5
3017.153	.890E-19	157.124 00 14004 000000_0	5 5F21	5 5F11	36 211	5
3017.223	.871E-19	219.937 00 14004 000000_0	5 6F11	5 5F21	36 211	5
3017.265	.104E-18	157.128 00 14004 000000_0	5 5F11	5 5F21	36 211	5
3017.345	.809E-19	219.941 00 14004 000000_0	5 6F21	5 5F11	36 211	5
3017.467	.142E-18	219.945 00 14004 000000_0	6 6A21	5 5A11	36 211	5
3017.711	.994E-19	104.773 00 14004 000000_0	4 4A21	4 4A11	36 211	5
3017.763	.411E-19	157.127 00 14004 000000_0	5 5 F1	5 5 F1	36 211	5
3017.884	.499E-19	164.776 00 14004 000000_0	4 4 F1	4 4 F1	36 211	5
3018.202	.110E-18	104.780 00 14004 000000_0	4 4F1	4 4F21	36 211	5
3018.241	.104E-18	52.576 00 14004 000000_0	3 3F21	3 3F11	36 211	5
3018.358	.109E-18	52.577 00 14004 000000_0	3 3F11	3 3F21	36 211	5
3018.528	.130E-18	52.578 00 14004 000000_0	3 3A11	3 3A21	36 211	5
3018.591	.454E-19	51.442 00 14004 000000_0	2 2 F1	2 2 F1	36 211	5
3018.655	.773E-19	51.442 00 14004 000000_0	2 2F11	2 2F21	36 211	5
3018.824	.559E-19	104.442 00 14004 000000_0	1 1F21	1 1F11	36 211	5
3019.002	.557E-21	6.0 0 0 14004 000000_0	1 0A21	2 0A11	36 311	5
3020.373	.105E-21	51.443 00 14004 000000_0	2 3F11	2 2F21	73 211	5
3020.391	.324E-21	645.054 00 14004 000000_0	1213A11	1212A21	73 211	5
3020.465	.275E-21	654.530 00 14004 000000_0	1112A11	1111A21	73 211	5
3020.557	.494E-21	52.572 00 14004 000000_0	3 4F11	3 3F21	73 211	5
3020.663	.224E-21	575.141 00 14004 000000_0	1011F13	1010F22	73 211	5
3020.743	.225E-21	684.980 00 14004 000000_0	1112F12	1111F23	73 211	5
3020.772	.105E-21	47.5773 00 14004 000000_0	910 F2	9 3 F1	73 211	5
3020.772	.439E-21	164.747 00 14004 000000_0	4 5F22	4 4F11	73 211	5
3020.802	.111E-21	47.5829 00 14004 000000_0	910F22	9 9F13	73 211	5
3020.812	.165E-21	52.571 00 14004 000000_0	3 4F21	3 3F11	73 211	5
3020.835	.714E-21	164.740 00 14004 000000_0	4 5 F1	4 4 F1	73 211	5
3020.861	.165E-21	376.743 00 14004 000000_0	8 9F12	5 4F21	73 211	5
3020.893	.165E-21	293.145 00 14004 000000_0	7 8F12	7 7F22	73 211	5
3020.893	.105E-21	689.545 00 14004 000000_0	1112F12	1111F22	73 211	5
3020.905	.275E-21	244.920 00 14004 000000_0	5 7F22	5 6F11	73 211	5
3020.932	.439E-21	376.742 00 14004 000000_0	8 9F23	5 4F12	73 211	5
3020.932	.494E-21	157.113 00 14004 000000_0	5 6F21	5 5F11	73 211	5
3020.955	.384E-21	293.141 00 14004 000000_0	7 8 F2	7 7 E1	73 211	5
3020.982	.275E-21	689.545 00 14004 000000_0	1112F12	1111F22	73 211	5
3021.012	.111E-21	376.741 00 14004 000000_0	8 9F22	5 4F11	73 211	5
3021.044	.124E-21	157.110 00 14004 000000_0	5 5F11	5 5F21	73 211	5
3021.057	.494E-21	212.548 00 14004 000000_0	5 7 F1	5 5 E1	73 211	5
3021.147	.154E-21	47.5829 00 14004 000000_0	910 F2	9 3A11	73 211	5
3021.161	.924E-21	212.548 00 14004 000000_0	5 7F11	5 4F21	73 211	5
3021.172	.111E-20	376.740 00 14004 000000_0	8 9F21	5 4A11	73 211	5
3021.172	.769E-21	293.140 00 14004 000000_0	7 4F22	7 7F11	73 211	5
3021.204	.105E-21	404.747 00 14004 000000_0	4 5F21	4 4F11	73 211	5
3021.273	.275E-21	61.445 00 14004 000000_0	1213A21	1212A11	73 211	5
3021.299	.224E-21	47.5829 00 14004 000000_0	910F21	9 9F13	73 211	5
3021.344	.297E-21	212.544 00 14004 000000_0	5 7A11	5 5A21	73 211	5
3021.374	.439E-21	293.140 00 14004 000000_0	7 4F21	7 7F12	73 211	5
3021.374	.439E-21	376.742 00 14004 000000_0	8 4F22	5 4F12	73 211	5
3021.382	.275E-21	684.951 00 14004 000000_0	1112F21	1111F11	73 211	5
3021.431	.104E-20	293.147 00 14004 000000_0	7 4F11	7 7F21	73 211	5
3021.441	.494E-21	47.5829 00 14004 000000_0	910F21	9 9F11	73 211	5
3021.441	.714E-21	376.741 00 14004 000000_0	8 4F22	5 4F11	73 211	5
3021.452	.275E-21	684.953 00 14004 000000_0	1112F11	1111F21	73 211	5
3021.472	.439E-21	575.042 00 14004 000000_0	1011-12	1010F21	73 211	5

Table 2. Results Obtained (Cont)

3021.495	.6042-21	370.713 00 14001 000000_0	8 9 F1	8 9 E1	73 211	6
3041.521	.6572-21	470.544 00 14001 000000_0	910F12	9 9F21	73 211	6
3041.545	.8542-21	575.015 00 14001 000000_0	1011A71	1010A21	73 211	6
3041.572	.1421-21					5
3041.732	.4142-2					5
3041.742	.1321-21					5
3041.752	.8742-14					5
3041.752	.1421-21					5
3041.753	.1742-21					5
3041.791	.4802-21					5
3042.057	.4802-21					5
3042.264	.1421-21					6
3043.127	.2132-21					6
3043.498	.9742-14	100.44-4 00 14001 000000_0	2 1F21	4 1F11	36 211	6
3043.498	.2802-21					5
3057.586	.8572-14	520.874 00 14001 000000_0	4 3A11	3 3A21	36 211	6
3057.741	.1172-14	520.875 00 14001 000000_0	4 3F21	3 3F11	36 211	6
3057.913	.1121-21	104.770 00 14001 000000_0	5 4 F1	4 4 E1	36 311	6
3057.962	.1422-21	104.773 00 14001 000000_0	5 4A11	4 4A11	36 311	6
3067.163	.1021-14	104.740 00 14001 000000_0	5 4F11	4 4F21	36 211	6
3067.235	.4572-14	104.770 00 14001 000000_0	5 4 E1	4 4 E1	36 211	6
3067.250	.1732-14	104.775 00 14001 000000_0	5 4F21	4 4F11	36 211	6
3067.249	.1172-14	104.773 00 14001 000000_0	5 4A21	4 4A11	36 211	6
3067.457	.1602-21	157.120 00 14001 000000_0	5 5F11	5 5F21	36 311	6
3076.075	.9172-14	157.120 00 14001 000000_0	5 5F11	5 5F21	36 211	6
3076.723	.1121-14	157.124 00 14001 000000_0	5 5F21	5 5F11	36 211	6
3076.907	.1622-21	249.920 00 14001 000000_0	7 6A11	6 5A21	36 311	6

Table 3. The Lines Unanalyzed Because of a Severe Blending

2917.653	00011001	00000000	910F13	1010F23	211
2917.662	00011001	00000000	910 E2	1010 E2	211
3013.711	00011001	00000000	9 9F21	9 9F11	211
3013.724	00011001	00000000	9 9F11	9 9F21	211
3014.735	00011001	00000000	8 8F22	8 8F11	211
3014.746	00011001	00000000	8 8 E2	8 8 E2	211
3017.815	00011001	00000000	4 4F21	4 4F11	211
3017.825	00011001	00000000	5 5F22	5 5F12	211
3048.153	00011001	00000000	3 2 E1	2 2 E1	211
3048.169	00011001	00000000	3 2F11	2 2F21	211

References

1. McClatchey et al (1973) AFCRL Atmospheric Absorption Line Parameters Compilation, AFCRL-TR-73-0096.
2. Fox, K. (1973) Analysis of Vibration-Rotation Spectra of Methane, AFCRL-TR-73-0738.
3. Pritchard et al (1973) Two-Meter Path Difference Interferometer for Fourier Spectroscopy, AFCRL-TR-73-0223.
4. Sakai, H. (1974) High-Resolution Fourier Spectroscopy, AFCRL-TR-74-0571.
5. Tarrago et al (1976) J. Mol. Spectrosc., 57:246.
6. Pine, A.S. (1976) J. Opt. Soc. Am., 66:97.

